Pergamon

Int. J. Solids Structures Vol. 32, No. 11, pp. 1501–1516, 1995

0020–7683/95 $9.50 + .00

0020–7683(94)00235–5

INTERACTIVE BUCKLING OF THIN-WALLED CLOSED ELASTIC BEAM-COLUMNS WITH INTERMEDIATE STIFFENERS

ZBIGNIEW KOLAKOWSKI
Department of Strength of Materials and Structures (K12), Technical University of Lodz, PL-90-924 Lodz, ul. Stefanowskiego 1/15, Poland

and

ANDRZEJ TETER
Department of Applied Mechanics, Technical University of Lublin, PL-20-618 Lublin, ul. Nadbystrzycka 36, Poland

(*Received* 13 *May* 1994; *in revised form* 15 *September* 1994)

Abstract—The design of thin-walled beam-columns must take into account the overall instability and the instability of component plates in the form of local buckling. This investigation is concerned with interactive buckling of thin-walled closed cross-section beam-columns with central intermediate stiffeners under axial compression and constant bending moment. The beams are assumed to be simply supported at the ends. The asymptotic expansion established by Byskov and Hutchinson is employed in the numerical calculations performed using the transition matrix method. The paper's aim is to contribute to the study of the equilibrium path in the post-buckling behaviour of imperfect structures using the first order approximation. The calculations are carried out for a few closed beam-columns.

NOTATION

a_{ijJ}	three-index coefficients in the nonlinear equilibrium equations by eqn (8) (Byskov and Hutchinson, 1977)
b_i	width of the *i*th wall of column
D_i	plate rigidity of the *i*th wall
E	Young's modulus
h_i	thickness of the *i*th wall of the column
l	length of the column,
m	number of axial half-waves of mode n
M_{ix}, M_{iy}, M_{ixy}	bending moment resultants for the *i*th wall
n	number of mode
N	number of interacting modes
$\bar{\mathbf{N}}$	force field,
N_{ix}, N_{iy}, N_{ixy}	in-plane stress resultants for the *i*th wall
N_{ix}°	pre-buckling in-plane stress for the *i*th wall
$N_{ix}^{(n)}, N_{iy}^{(n)}, N_{ixy}^{(n)}$	in-plane stress resultants for the *i*th wall in the first approximation,
N_{iy}^{*}	eqn (A2)
N_{ixy}^{*}	eqn (A2)
Q_{iy}^{*}	eqn (A2)
$\bar{\mathbf{U}}$	displacement field
u_i, v_i, w_i	displacement components of middle surface of the *i*th wall
$u_i^{\circ}, v_i^{\circ}, w_i^{\circ}$	pre-buckling displacement fields
$u_i^{(n)}, v_i^{(n)}, w_i^{(n)}$	buckling displacement fields
Δ_i	measure of the applied pressure
λ	scalar load parameter
λ_n	value of λ at bifurcation mode number n
λ_s	maximum value of λ for imperfect column
ν	Poisson's ratio ($\nu = 0.3$),
ξ_n	amplitude buckling mode number n
$\bar{\xi}_n$	imperfection amplitude corresponding to ξ_n
$\sigma_n^* = \sigma_n 10^3/E$	dimensionless stress of mode number n, $\sigma_m^* = \min(\sigma_1^*, \sigma_2^*, \sigma_3^*)$
σ_s^*	limit dimensionless stress for imperfect column (load-carrying capacity)
ζ_i	x_i/b_i
η_i	y_i/b_i.

1. INTRODUCTION

Intermediate stiffeners are widely used in many types of metal structures. These stiffeners carry a portion of the loads and sub-divide the plate element into smaller sub-elements, thus considerably increasing the load-carrying capacity. The size and position of intermediate stiffeners in thin-walled structures exerts a strong influence on the buckling and post-buckling behaviour of the thin-walled structures.

Thin-walled structures consisting of plate elements having a number of buckling modes differing from one another both in quantitative (e.g. by the number of half-waves) and in qualitative (e.g. by global and local buckling) respects. In the case of finite displacements, different buckling modes are interrelated, even with loads close to their critical values (eigenvalues of a respective boundary problem). The investigation of stability of equilibrium states requires an application of a non-linear theory that enables us to estimate the influence of different factors on the structure's behaviour.

One of the most important problems in the investigation of the stability of these structures is the interaction of various buckling modes (the so-called coupled buckling).

The allowance for interactive buckling is necessary for the determination of limiting load capacity and of the imperfection sensitivity of structures close to optimum, where the values of critical loads are identical or nearly so. In the case when the post-buckling behaviour of each mode taken separately is stable, their interaction may result in unstable behaviour and, consequently, in greater imperfection sensitivity.

The concept of interactive buckling involves the general asymptotic theory of stability. Among all versions of the general non-linear theory, the Koiter theory (1963, 1976) of conservative systems is most popular owing to its general character and development, even more so after Byskov and Hutchinson (1977) formulated it in a convenient way. The theory is based on asymptotic expansions of the post-buckling path and is capable of considering nearly simultaneous buckling modes. The expression for potential energy of the system expands in a series relative to the amplitudes of linear modes near the point of bifurcation; the latter generally corresponds to the minimum value of critical load (the so-called bifurcation load).

For the first order approximation Koiter and van der Neut (1980) have proposed a technique in which the interaction of an overall mode with two local modes (three-mode approach) having the same wavelength has been considered. The fundamental mode is henceforth called "primary" and the non-trivial higher local mode (having the same wavelength as the "primary") corresponding to the mode triggered by overall longwave mode is called "secondary". The local secondary buckling mode is analogous to the mixed one; thus, its consideration in the first approximation enables us to neglect the second order mixed modes (Koiter and van der Nuet, 1980; Kolakowski, 1993a,b; Krolak, 1990; Manevich, 1988; Pignataro and Luongo, 1987a,b; Sridharan and Peng, 1989).

Numerical calculations by Kolakowski (1988, 1989b,c) have proved that the interaction of local modes having considerably different wavelengths is either very weak or does not occur at all. Moreover, one can see that the interaction of two global modes of buckling is very weak or does not occur at all. According to the assumptions mode in Byskov and Hutchinson's theory (1977), local buckling modes do not interact explicitly. However, the interaction occurs through the interaction of each of them with the global mode. It can be noticed that the Euler buckling can interact with an even number of local modes—symmetric or antisymmetric, but the flexural–torsional mode only with pairs of symmetric and antisymmetric modes [see Sridharan and Ali (1986), Pignataro and Luongo (1987a,b), and Kolakowski (1989a) for more detailed analysis]. The problem of the interaction of the global mode with the local ones is of great significance. This effect is contained in the term $\sigma_1 l_{11}(u_j, u_k)$ where $j, k = 2,3$ (where the index is 1 for the global mode, 2 for the primary local buckling mode and 3 for the secondary local mode having the same number of half-waves as the primary one) in coefficients $a_{ijJ} \neq 0$ of the equations (8), and in the others $a_{ijJ} = 0$. In order to find the most unfavourable second local buckling mode, several first values of local stresses, corresponding to a given number of half waves m, must be determined. Then the coefficients a_{ijJ} for each of these values are calculated.

In the energy expression for the first order approximation the coefficients of the cubic terms $\xi_1\xi_2^2$, $\xi_1\xi_3^2$ and $\xi_1\xi_2\xi_3$ are the key terms governing the interaction. In the case of disregarding the interaction between overall mode, the primary local mode and the secondary local mode, the coefficient of the $\xi_1\xi_2\xi_3$ term in the energy expression vanishes. In the analysis of the column with doubly symmetric cross-sections the coefficients of the $\xi_1\xi_2^2$ and $\xi_1\xi_3^2$ terms—the coefficients a_{ijJ} of the non-linear system (8)—vanish.

In some cases an improper selection of mode, even if a few of them are considered, may lead to an overestimation of the construction's load-carrying capacity; also, the consideration of the two-mode approach may sometimes be misleading and yield false conclusions. This can be accomplished only by means of non-linear analysis (Kolakowski, 1989a).

A more comprehensive review of the literature concerning interactive buckling has been done by Ali and Sridharan (1988), Benito and Sridharan (1984–85), Manevich (1985, 1988), Moellmann and Goltermann (1989), Pignataro and Luongo (1987a,b), Sridharan and Ali (1985, 1986), Sridharan and Peng (1989), Tvergaard (1973) and Kolakowski (1987a,b, 1989a–c).

The importance of the minimum rigidity of the intermediate stiffeners required to restrict buckling to the plate elements was studied by Timoshenko (1921), Barbré (1936), Cox and Riddell (1949), Desmond (1977), Höglund (1978), Konig (1978) and others. The test specimens, experimental works and comparisons made with design rules of plates and open cross-section structures were detailed by Hoon *et al.* (1993) and Bernard *et al.* (1993).

Mathematical models tend to a higher precision and closer approximation of real structures, which enable us to analyse more exactly the phenomena occurring during and after the loss of stability. Therefore, a precise determination of eigenvalues and eigenmodes for different buckling modes is an importent factor enabling a more detailed analysis of the structure's behaviour.

A rapid development of science and technology, as well as a widespread use of computer-aided methods (CAD/CAM), enables improved structure design; in accordance with the theory of catastrophes, these structures show singularities of increasing order. The safety and reliability requirements of thin-walled structures are also more rigorous and can be matched only if investigations are carried out continuously (Kolakowski, 1994).

In the present paper, the post-buckling behaviour of thin-walled structures with intermediate stiffeners in the elastic range under axial compression and a bending moment is examined on the basis of Byskov and Hutchinson's method, with co-operation between all the walls of the structures being taken into account. The study is based on the numerical method of the transition matrix by Unger (1969), Klöppel and Bilstein (1971) and Bilstein (1974) using the Godunov orthogonalization method (Bidermann, 1977). Each wall has a central intermediate stiffener.

The influence of number of half-waves m for assumed imperfections on the load-carrying capacity is neglected, as distinct from the papers by Manevich (1982) and Kolakowski (1988, 1989a–c, 1993a,b).

The most important advantage of this method is that it enables us to describe a complete range of behaviour of thin-walled structures from global to local stability. In the solution obtained, the effects of interaction of certain modes having the same wavelength, the shear lag phenomenon and also the effect of cross-sectional distortions are included.

Since for the first order approximation the limit load is always lower than the minimum value of a bifurcational load obtained in the linear analysis, this approximation can be used as a lower bound estimation of load-carrying capacity.

2. STRUCTURAL PROBLEM

Long thin-walled prismatic beam-columns of length l, composed of plane, rectangular plate segments interconnected along longitudinal edges, simply supported at both ends, are considered.

The cross-section of this structure, composed of several plates, as well as local Cartesian coordinate systems are presented in Fig. 1.

A plate model is adopted for the beam-column. For the ith wall precise geometrical relationships are assumed to take into account both out-of-plane and in-plane bending:

$$\begin{aligned} \varepsilon_{ix} &= u_{i,x}+0.5(u_{i,x}^2+v_{i,x}^2+w_{i,x}^2) \\ \varepsilon_{iy} &= v_{i,y}+0.5(u_{i,y}^2+v_{i,y}^2+w_{i,y}^2), \\ 2\varepsilon_{ixy} &= \gamma_{ixy} = u_{i,y}+v_{i,x}+u_{i,x}u_{i,y}+v_{i,x}v_{i,y}+w_{i,x}w_{i,y}, \\ \ae_{ix} &= -w_{i,xx}, \quad \ae_{iy} = -w_{i,yy}, \quad \ae_{ixy} = -w_{i,xy}. \end{aligned} \tag{1}$$

The differential equilibrium equations resulting from the virtual work principle corresponding to expressions (1) for the ith wall can be written as follows:

$$\begin{aligned} N_{ix,x}+N_{ixy,y}+(N_{ix}u_{i,x})_{,x}+(N_{iy}u_{i,y})_{,y}+(N_{ixy}u_{i,x})_{,y}+(N_{ixy}u_{i,y})_{,x} &= 0, \\ N_{iy,y}+N_{ixy,x}+(N_{ix}v_{i,x})_{,x}+(N_{iy}v_{i,y})_{,y}+(N_{ixy}v_{i,x})_{,y}+(N_{ixy}v_{i,y})_{,x} &= 0, \\ D_i\nabla\nabla w_i-(N_{ix}w_{i,x})_{,x}-(N_{iy}w_{i,y})_{,y}-(N_{ixy}w_{i,x})_{,y}-(N_{ixy}w_{i,y})_{,x} &= 0. \end{aligned} \tag{2}$$

The solution of these equations for each plate should satisfy kinematic and static conditions at the junctions of adjacent plates and boundary conditions at the ends $x = 0$ and $x = l$ (see Appendix A).

The non-linear problem is solved by the asymptotic Byskov and Hutchinson method (1977). Displacement $\bar{\mathbf{U}}$ and force $\bar{\mathbf{N}}$ fields are expanded in power series in the buckling mode amplitudes, ξ_n (divided by the thickness of the first component plate):

$$\begin{aligned} \bar{\mathbf{U}} &= \lambda\bar{\mathbf{U}}_i^{(0)}+\xi_n\bar{\mathbf{U}}_i^{(n)}+\cdots \\ \bar{\mathbf{N}} &= \lambda\bar{\mathbf{N}}_i^{(0)}+\xi_n\bar{\mathbf{N}}_i^{(n)}+\cdots, \end{aligned} \tag{3}$$

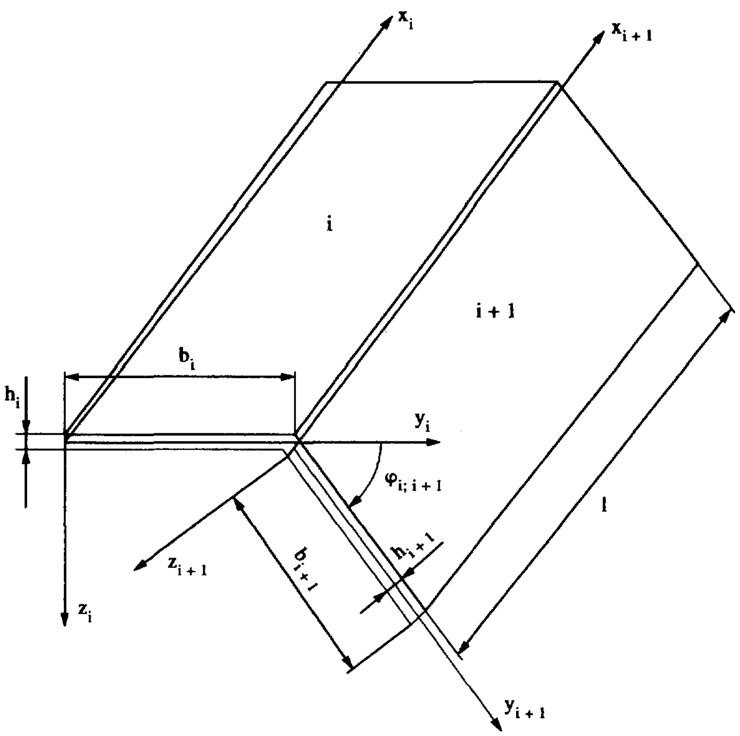

Fig. 1. Prismatic plate structure and the local coordinate system.

where the pre-buckling fields are $\bar{\mathbf{U}}_i^{(0)}$, $\bar{\mathbf{N}}_i^{(0)}$ and the buckling modes $\bar{\mathbf{U}}_i^{(n)}$, $\bar{\mathbf{N}}_i^{(n)}$. In eqns (3), ξ_n is the amplitude of the nth buckling mode. The range of indices is $[1, N]$, where N is the number of interacting modes.

By substituting the expansion (3) into equations of equilibrium (2), junction conditions (A1) and boundary conditions (A3), boundary problems of zero and first order can be obtained. The zero approximation describes the pre-buckling state, while the first approximation, i.e. the linear problem of stability which enables us to determine the critical value and the buckling mode, is reduced to a system of homogeneous differential equations.

The plates with linearly varying stresses along their widths are divided into several strips under uniformly distributed compression (tension) stresses (Fig. 2). As distinct from the finite strips method, the exact transition matrix method is used in this case.

The pre-buckling solution consisting of homogeneous fields is assumed as:

$$
\begin{aligned}
u_i^0 &= -x_i\Delta_i,\\
v_i^0 &= \nu y_i\Delta_i,\\
w_i^0 &= 0,
\end{aligned}
\tag{4}
$$

where Δ_i is the actual loading. This loading is specified as the product of a unit loading system and a scalar load factor Δ_i.

As the intermediate stiffeners are taken into consideration, numerical difficulties connected with convergance of the presented problem appear contrary to the papers by Kolakowski (1989a, 1993a, b). These difficulties induce the necessity of introducing new orthogonal functions in the sense of boundary conditions for two longitudinal edges (see Appendix B):

$$
\begin{aligned}
\bar{a}_i^{(n)} &= N_{iy}^{*(n)}(1-\nu^2)/(Eh_i) = (1+2\nu\lambda\Delta_i)v_{i,\eta}^{(n)}+\nu(1+\nu\lambda\Delta-\lambda\Delta_i)u_{i,\zeta}^{(n)},\\
\bar{b}_i^{(n)} &= N_{ixy}^{*(n)}(1+\nu^2)/(Eh_i) = 0.5(1-\nu)[(1-2\lambda\Delta_i)u_{i,\eta}^{(n)}+(1+\nu\lambda\Delta_i-\lambda\Delta_i)v_{i,\zeta}^{(n)}],\\
\bar{c}_i^{(n)} &= u_i^{(n)},\\
\bar{d}_i^{(n)} &= v_i^{(n)},\\
\bar{e}_i^{(n)} &= w_i^{(n)},\\
\bar{f}_i^{(n)} &= w_{i,\eta}^{(n)},\\
\bar{g}_i^{(n)} &= -M_{iy}^{(n)}/D_i = w_{i,\eta\eta}^{(n)}+\nu w_{i,\zeta\zeta}^{(n)},\\
\bar{h}_i^{(n)} &= -Q_{iy}^{*(n)}/D_i = w_{i,\eta\eta\eta}^{(n)}+(2-\nu)w_{i,\zeta\zeta\eta}^{(n)},
\end{aligned}
\tag{5}
$$

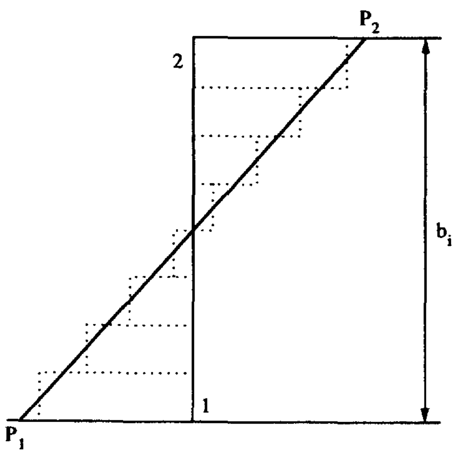

Fig. 2. Discretization of a linear distribution of stresses by means of finite strips.

where $(..)_{i,\zeta} = \partial(..)/\partial\zeta_i$, $(..)_{i,\eta} = \partial(..)/\partial\eta_i$. Considering the above system of differential equations (2), the first approximation may be written in the form:

$$\bar{a}^{(n)}_{i,\eta} = (1-v^2)\lambda\Delta_i\bar{d}^{(n)}_{i,\zeta\zeta} - 0.5(1-v)(1+v\lambda\Delta_i - \lambda\Delta_i)\bar{c}^{(n)}_{i,\zeta\eta} - 0.5(1-v)(1+2v\lambda\Delta_i)\bar{d}^{(n)}_{i,\zeta\zeta},$$
$$\bar{b}^{(n)}_{i,\eta} = -\bar{c}^{(n)}_{i,\zeta\zeta} + (3-v^2)\lambda\Delta_i\bar{c}^{(n)}_{i,\zeta\zeta} - v\bar{d}^{(n)}_{i,\zeta\eta} + v(1-v)\lambda\Delta_i\bar{d}^{(n)}_{i,\zeta\eta},$$
$$\bar{c}^{(n)}_{i,\eta} = [2\bar{b}^{(n)}_i/(1-v) - (1+v\lambda\Delta_i - \lambda\Delta_i)\bar{d}^{(n)}_{i,\zeta}]/(1-2\lambda\Delta_i),$$
$$\bar{d}^{(n)}_{i,\eta} = [\bar{a}^{(n)}_i - v(1+v\lambda\Delta_i - \lambda\Delta_i)\bar{c}^{(n)}_{i,\zeta}]/(1+2v\lambda\Delta_i),$$
$$\bar{e}^{(n)}_{i,\eta} = \bar{f}^{(n)}_i,$$
$$\bar{f}^{(n)}_{i,\eta} = \bar{g}^{(n)}_i - v\bar{e}^{(n)}_{i,\zeta\zeta},$$
$$\bar{g}^{(n)}_{i,\eta} = \bar{h}^{(n)}_i - 2(1-v)\bar{f}^{(n)}_{i,\zeta\zeta},$$
$$\bar{h}^{(n)}_{i,\eta} = -v\bar{f}^{(n)}_{i,\zeta\zeta\eta} - \bar{e}^{(n)}_{i,\zeta\zeta\zeta\zeta} - Eh_ib_i^2\lambda\Delta_i\bar{e}^{(n)}_{i,\zeta\zeta}/D_i. \qquad (6)$$

The first order solutions may be formulated as follows:

$$\bar{a}^{(n)}_i = \bar{A}^{(n)}_i(\eta)\sin\frac{m\pi\zeta b_i}{l},$$
$$\bar{b}^{(n)}_i = \bar{B}^{(n)}_i(\eta)\cos\frac{m\pi\zeta b_i}{l},$$
$$\bar{c}^{(n)}_i = \bar{C}^{(n)}_i(\eta)\cos\frac{m\pi\zeta b_i}{l},$$
$$\bar{d}^{(n)}_i = \bar{D}^{(n)}_i(\eta)\sin\frac{m\pi\zeta b_i}{l},$$
$$\bar{e}^{(n)}_i = \bar{E}^{(n)}_i(\eta)\sin\frac{m\pi\zeta b_i}{l},$$
$$\bar{f}^{(n)}_i = \bar{F}^{(n)}_i(\eta)\sin\frac{m\pi\zeta b_i}{l},$$
$$\bar{g}^{(n)}_i = \bar{G}^{(n)}_i(\eta)\sin\frac{m\pi\zeta b_i}{l},$$
$$\bar{h}^{(n)}_i = \bar{H}^{(n)}_i(\eta)\sin\frac{m\pi\zeta b_i}{l}. \qquad (7)$$

$\bar{A}^{(n)}_i, \bar{B}^{(n)}_i, \bar{C}^{(n)}_i, \bar{D}^{(n)}_i, \bar{E}^{(n)}_i, \bar{F}^{(n)}_i, \bar{G}^{(n)}_i$ and $\bar{H}^{(n)}_i$ (with the mth harmonic) are initially unknown functions that will be determined by the numerical method of transition matrices. The system of ordinary differential equations for the first order with appropriate junction conditions for adjacent plates is solved by the transition matrices method using numerical integration of the equilibrium equations in the transverse direction in order to obtain a relation between state vectors on two longitudinal edges, applying the Godunov orthogonalization method (Bidermann, 1977).

The omission of the displacements of the fundamental state implies that we ignore the difference between configurations of the undeformed state and the fundamental state, and we may consequently regard the previously defined displacements u^0_i, v^0_i as additional ones from the fundamental state to the adjacent state.

The assumed fields for the first order non-linear approximation ensure compatibility of the corner displacements of the constituent plates. Thus, $v = 0$ at the ends, implying that the plates are restrained in their plane at the ends. The point of major interest is that this method can be employed to study the effect on the post-buckling stiffness of enforcing the compatibility of the displacements in the cross-sectional plane at the corners [for more detailed analysis see Sridharan and Graves-Smith (1981)].

The global buckling mode occurs at $m = 1$ and the local modes at $m > 1$ (with $b_i \ll l$). Each buckling mode is normalized so that the maximum normal displacement is equal to the thickness of the first constituent wall.

At the point where the load parameter λ_s reaches its maximum value for an imperfect structure (secondary bifurcation or limit points), the Jacobian of a non-linear system of equations (Byskov and Hutchinson, 1977):

$$\left(1-\frac{\lambda}{\lambda_J}\right)\xi_J + a_{ijJ}\xi_i\xi_j + \cdots = \frac{\lambda}{\lambda_J}\bar{\xi}_J \quad \text{at} \quad J = 1, 2, \ldots, N \tag{8}$$

is equal to zero.

The expression for a_{ijJ} is given in Appendix C. The formulae for the post-buckling coefficients a_{ijJ} involve only the buckling modes. The result of integration along x indicates that the post-buckling coefficients a_{ijJ} are zero when the sum of the wave numbers associated with the three modes $(m_i + m_j + m_J)$ is even.

3. ANALYSIS OF RESULTS

The theory presented in this paper, as applied to the full strain tensor of thin-walled plates (1), shows a very good compatibility in comparison with earlier results obtained by Kolakowski (1989a,c, 1993a,b), having omitted the terms $0.5u_{i,x}^2$, $0.5v_{i,y}^2$ and $(u_{i,x}u_{i,y} + v_{i,x}v_{i,y})$ in expressions for ε_{ix}, ε_{iy} i $2\varepsilon_{ixy} = \gamma_{ixy}$, respectively.

The long thin-walled prismatic beam-columns of square cross-section (Fig. 3a), with corners bevelled at an angle of 45° (Fig. 3b) reinforced with V- and C-shaped central intermediate stiffeners (Fig. 3c and d, respectively) have been performed. Bevelled corners and intermediate stiffeners were made up of plates whose width is b_s. Detailed numerical

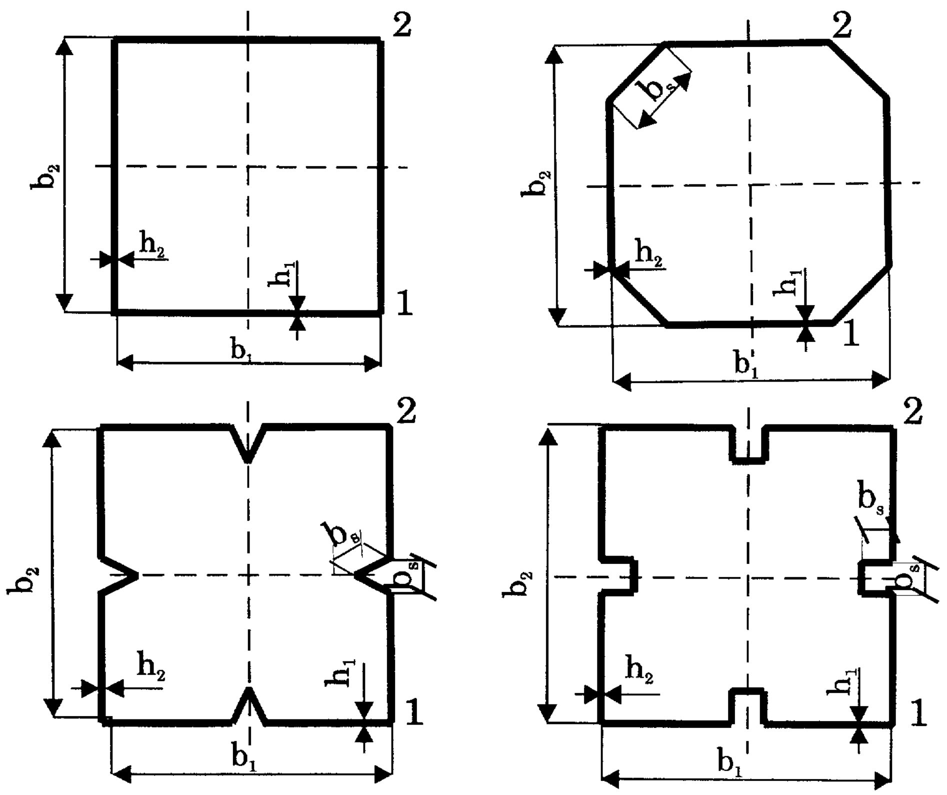

Fig. 3. Types of closed cross-section considered.

calculations have been carried out for several different sizes of cross-sectional reinforcements of thin-walled beam-columns subject to uniform and eccentric compression.

In the pre-buckling state, the beam-column is subjected to linearly variable stresses caused by axial forces and bending moments which are dealt with as external loads. The load distribution can be described by the ratio of stress $p_j(y)$ at point "j" of cross-section to the greatest compressive stress, $p_{max} = p_1$, applied to the bottom flange (Fig. 3). In the present paper the load distribution is defined as the ratio of stresses in the top flange (point 2) to maximum stresses in the bottom flange, $\varkappa = p_2/p_{max} = p_2/p_1$. Stress p_j is considered positive if it is a compressive stress. In order to compare load capacities of different cross-sections (Fig. 3a–f), identical distributions of external stress are assumed; this implies a change in the values of compressive force and bending moment.

The calculations are carried out for a beam-column of the following geometrical dimensions (Fig. 3a):

$$b_1/b_2 = 1.0, \quad h_1/h_2 = 1.0, \quad l/b_2 = 27.5, \quad b_1/h_1 = 100.$$

Intermediate stiffeners are modelled with plates, their dimensions being $b_s/h_1 = \{4, 6, 8, 10, 12\}$; correspondingly, for bevelled corners $b_s/h_1 = \{9, 18, 27, 36\}$. Figures 4–9 present dimensionless critical stress, σ_n^*, as a function of the number of half-waves, m, for the above values of b_s/h_1. As a comparison, the results are shown as obtained for a "smooth" square column [i.e. $b_s/h_1 = 0$, Figs 4(0)–9(0)]. A modification of a square cross-section (Fig. 3a) accomplished by corner bevelling (Fig. 3b) results in the expected increase in the local critical stress value owing to the increase of flexural rigidity of component plates, and in a slight decrease in global critical stress value (up to about 10%) due to the reduced moment of inertia of the cross-section. The introduction of intermediate stiffeners increases the flexural rigidity of plate elements and, consequently, also the local critical stress values. Global critical stress values for all analysed types of intermediate stiffeners remain virtually unchanged because of the small variations in the moment of inertia of the cross-section. Regarding global stability, a less favourable case is bevelled corners, which reduce the moment of inertia of the cross-section to a greater extent than intermediate stiffeners.

Columns reinforced with intermediate stiffeners may show two local minima for two different local buckling modes (Figs 6–9). The first one refers to the smaller number of half-waves ($m = 7$–13) and the second one to the greater number of half-waves ($m = 66$–77) as compared with the column without reinforcement. In particular cases the values of these minima for local buckling modes can be almost equal [Figs 6(12), 7(10), 8(8) and 9(8)].

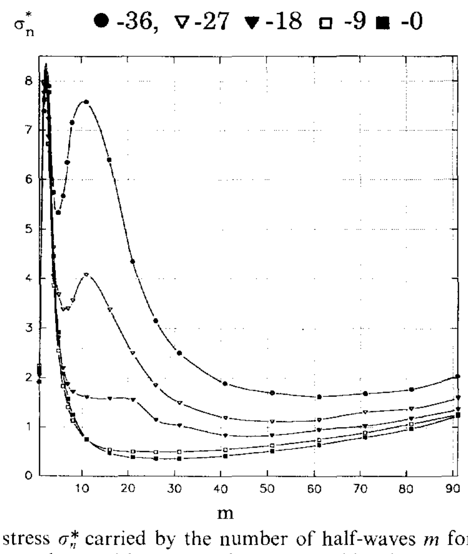

Fig. 4. Dimensionless stress σ_n^* carried by the number of half-waves m for uniform compression column with cross-section presented in Fig. 3b.

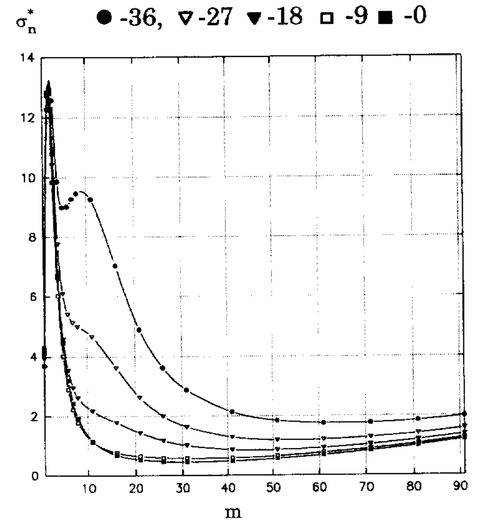

Fig. 5. Dimensionless stress σ_n^* carried by the number of half-waves m for eccentrically compressed column ($\varpi = 0$) with cross-section presented in Fig. 3b.

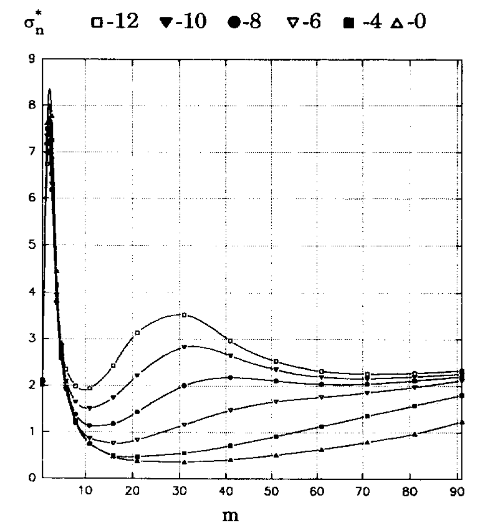

Fig. 6. Dimensionless stress σ_n^* carried by the number of half-waves m for uniform compression column with cross-section presented in Fig. 3c.

Each minimum, however, corresponds to a different local buckling mode. Primary and secondary local buckling modes referring to these two minima for a column under uniform compression ($\varpi = 1$) ($b_s/h_1 = 12$) are shown in Figs 10 and 11. Special attention should be paid to the fact that critical stress values referring to the second minimum are nearly equal for both local modes. In the paper of Bernard *et al.* (1993), the local buckling modes presented in Figs 10 and 11 are named as follows: $\sigma_1^* = 1.114$ ($m = 13$), local distortional buckling mode (Fig. 10); $\sigma_2^* = 2.033$ ($m = 66$), local antisymmetric mode (Fig. 11); $\sigma_3^* = 2.042$ ($m = 66$), local symmetric mode (Fig. 11). The local mode $\sigma_3^* = 1.650$ ($m = 13$) illustrated in Fig. 10, which may be named the local bending mode, is analogous to that of a "smooth" column, $\sigma_3^* = 0.52336$ ($m = 27$) [Figs 6(0) and 8(0)] [see Sridharan and Ali (1986), and Kolakowski (1989a, c)].

For $b_s/h_1 \geqslant 6$, the intermediate stiffeners do not practically contribute to any increase in local critical stress values corresponding to the second minimum ($m = 66$–77; Figs 6–9). The theory presented here enables us to carry out an analysis of all buckling modes for intermediate stiffeners of different shapes and flexural rigidities; this can help in their rational design. Too small sizes of intermediate stiffeners [e.g. V-shaped stiffeners, $b_s/h_1 = 4$;

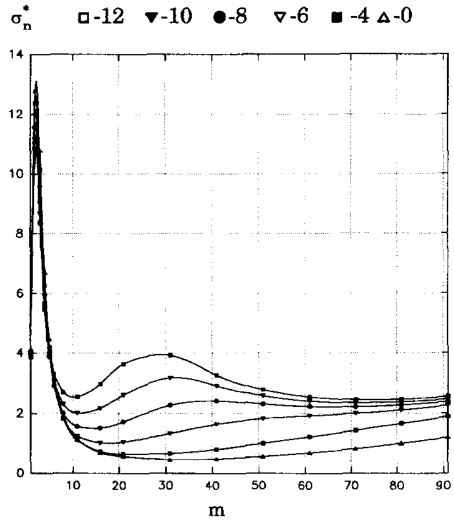

Fig. 7. Dimensionless stress σ_n^* carried by the number of half-waves m for eccentrically compressed column ($\varkappa = 0$) with cross-section presented in Fig. 3c.

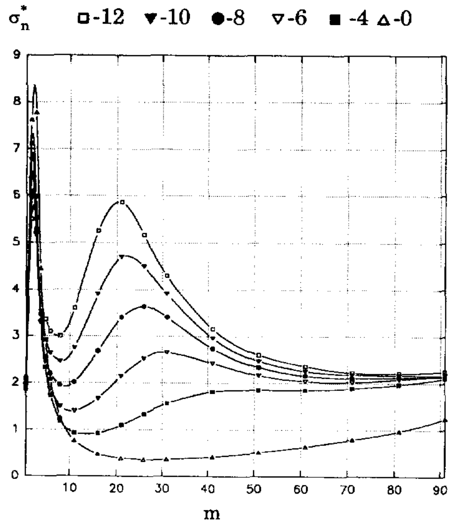

Fig. 8. Dimensionless stress σ_n^* carried by the number of half-waves m for uniform compression column with cross-section presented in Fig. 3d.

Fig. 6(4)], with their low flexural rigidity, cause virtually no increase in the critical stress values. Higher eccentricity of compressive force may increase local critical stress values, σ_2^*, by up to 20% due to higher stability coefficients of the webs and top flange (Table 1; compare cases 1 and 8; 4 and 9; 5 and 10; 6 and 11); moreover, it strongly influences the global stress values, σ_1^*. For eccentric compression ($\varkappa = 0$), global critical stresses are almost doubled (Table 1; compare cases 1 and 8; 4 and 9).

Buckling modes for eccentrically compressed beam-columns of sizes discussed above are presented in Figs 12 and 13.

Detailed numerical calculations aiming at the determination of the load-carrying capacity of the structures with imperfections are carried out for the following column dimensions:

$$b_1/b_2 = 1, \quad h_1/h_2 = 1, \quad l/b_2 = 27.5, \quad b_1/h_1 = 100,$$

having assumed the following imperfections: $|\bar{\xi}_1| = 1.0$, $|\bar{\xi}_2| = 0.2$, $\bar{\xi}_3 = 0.0$.

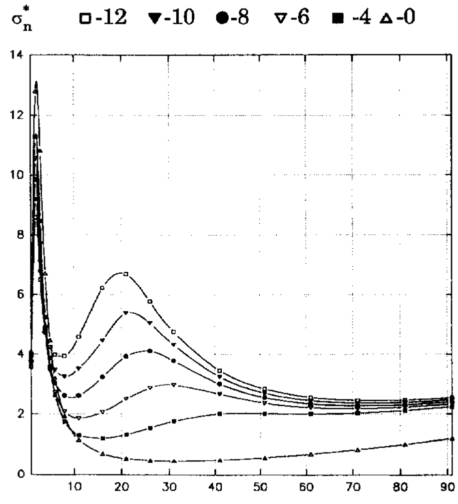

Fig. 9. Dimensionless stress σ_n^* carried by the number of half-waves m for eccentrically compressed column ($\varkappa = 0$) with cross-section presented in Fig. 3d.

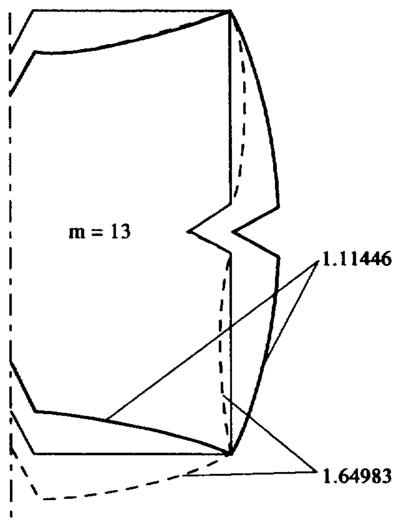

Fig. 10. Two local modes at $m = 13$ for uniform compression column.

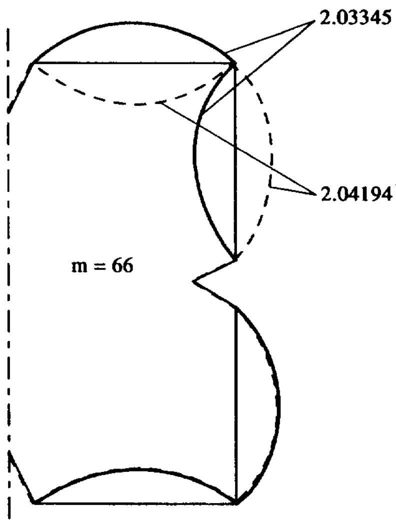

Fig. 11. Two local modes at $m = 66$ for uniform compression column.

Table 1. Load-carrying capacity for beam-column with cross-section presented in Fig. 3c at imperfections $|\bar{\xi}_1| = 1.0$, $|\bar{\xi}_2| = 0.2$, $\bar{\xi}_3 = 0.0$

	b_s/h_1	κ	σ_1^*	σ_2^*	σ_3^*	σ_s^*/σ_m^*
1	0	1	2.13500(1)	0.36154(27)	0.52336(27)	0.8265
2	8	1	2.07383(1)	1.11446(13)	1.64983(13)	0.9111
3	8	1	2.07383(1)	2.03345(66)	2.04194(66)	0.6661
3a	8	1	2.07383(1)	2.04194(66)	2.03345(66)	0.6650
4	10	1	2.04690(1)	1.50197(11)	2.19070(11)	0.9081
5	10	1	2.04690(1)	2.15782(70)	2.17214(70)	0.6894
5a	10	1	2.04690(1)	2.17214(70)	2.15782(70)	0.6881
6	12	1	2.01722(1)	1.91049(10)	2.71318(10)	0.8777
7	12	1	2.01722(1)	2.25643(72)	2.27299(72)	0.7199
7a	12	1	2.01722(1)	2.27299(72)	2.25643(72)	0.7185
8	0	0	4.23660(1)	0.46196(32)	1.05586(32)	0.7409
9	10	0	4.05580(1)	1.98805(12)	4.95936(12)	0.8837
10	10	0	4.05580(1)	2.34130(72)	3.49264(72)	0.7021
11	12	0	3.99622(1)	2.52131(10)	6.27080(10)	0.8922
12	12	0	3.99622(1)	2.44594(74)	3.62682(74)	0.7005

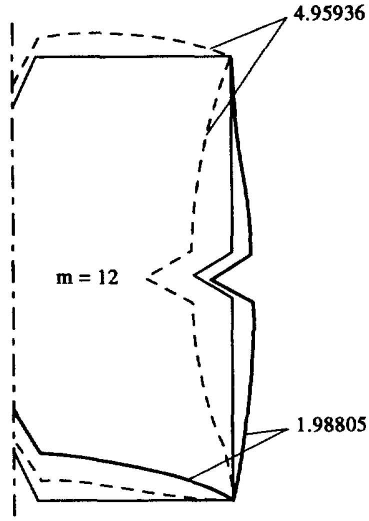

Fig. 12. Two local modes at $m = 12$ for eccentrically compressed column ($\varkappa = 0$).

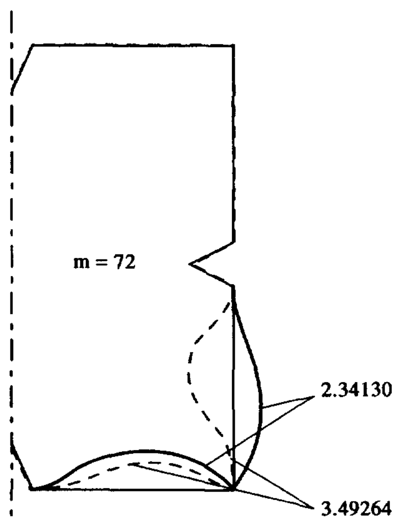

Fig. 13. Two local modes at $m = 72$ for eccentrically compressed column ($\varkappa = 0$).

In each case the signs of the imperfections have been chosen in the most unfavourable fashion, i.e. so that σ_s^*would assume its minimum value [see Manevich (1982) and Kolakowski (1987a, 1989a, c) for a more detailed discussion].

The local mode imperfections always promote an interaction between the local modes and the global mode.

Tables 1 and 2 present the values of dimensionless critical stresses, σ_n^* (the corresponding numbers of half-waves, m, are given in parentheses) and the load-carrying capacity to minimum critical stress ratios, σ_s^*/σ_m^*. The cases of uniform ($\varkappa = 1$) and eccentric ($\varkappa = 0$) compression are analysed. It should be noted that in the determination of load-carrying capacity imperfections are assumed for the global mode $\bar{\zeta}_1$ and for only one of the local buckling modes $\bar{\zeta}_2$ (σ_1^* and σ_2^* in Tables 1 and 2).

In Table 2 a result is given for a beam-column with corners bevelled at 45°, its dimensions being $b_s/h_1 = \{27, 36\}$. It is evident that when critical stress values become close to each other, the imperfection sensitivity increases (compare cases 2 and 3 in Table 2); this is substantiated by earlier papers of the first author. A decrease of limit load in the presence of imperfections is very significant, especially if local imperfections are present. Attention should be paid to the proper selection of local buckling modes (compare cases 2 and 2a; 3 and 3a). This can be accomplished only by means of non-linear analysis.

Table 1 presents results of calculations carried out for V-stiffened beam-columns, its dimensions being $b_s/h_1 = \{8, 10, 12\}$. These data allow us to conclude that an interaction of global buckling mode with local symmetric mode and local antisymmetric mode (cases 3a, 5a, 7a) is more dangerous than with the local distortional mode and the local bending mode (cases 2, 4, 6) or with the local antisymmetric and local symmetric modes (cases 3, 5, 7).

In the case of eccentric compression the global stress values, σ_1^*, are significantly higher than under uniform compression, while the limit stress values, σ_s^*/σ_m^* are similar (compare, for example, cases 3 and 5 in Table 2); this means that the imperfection sensitivity increases together with the eccentricity of compressive force.

The interaction of global buckling mode with two local modes corresponding to the second local minimum ($m = 72$–74) is more dangerous than with local modes related to the first minimum ($m = 10$–12) (compare cases 9 and 10 and cases 11 and 12 in Table 1).

Results obtained for intermediate C-stiffeners are analogous to those for V-stiffeners.

The modification of cross-section (Fig. 3b–f) makes the load-carrying capacity greater than in the case of a "smooth" beam-column. Much regard has to be paid, however, to the proper choice of flexural rigidity of plate elements and to the cross-sectional moment of inertia, as well as to the correct determination of their load-carrying capacity.

The present theory enables us to carry out a full analysis of interactive buckling in beam-columns subject to eccentric compression, making allowance for global pre-buckling bending; at this point it differs from the approximate analysis presented by Roorda (1988), where only global bending was considered.

4. CONCLUSIONS

The interactive buckling analysis of thin-walled closed beam-columns with central intermediate stiffener on each plate under axial compression and constant bending moment

Table 2. Load-carrying capacity for beam-column with cross-section presented in Fig. 3b at imperfections $|\bar{\zeta}_1| = 1.0$, $|\bar{\zeta}_2| = 0.2$, $\bar{\zeta}_3 = 0.0$

	b_s/h_1	κ	σ_1^*	σ_2^*	σ_3^*	σ_s^*/σ_m^*
1	0	1	2.13500(1)	0.36154(27)	0.52336(27)	0.8265
2	27	1	2.05107(1)	1.12413(52)	1.18228(52)	0.7422
2a	27	1	2.05107(1)	1.18228(52)	1.12413(52)	0.7942
3	36	1	1.91603(1)	1.62832(60)	1.74362(60)	0.7124
3a	36	1	1.91603(1)	1.74362(60)	1.62832(60)	0.7654
4	0	0	4.23660(1)	0.46196(32)	1.05586(32)	0.7409
5	36	0	3.80155(1)	1.74269(64)	3.37900(64)	0.7275

carried out by means of the transition matrix method has been presented. Global and local modes are described by plate theory. Intermediate stiffeners are found to exert a strong influence on the local buckling modes.

The applied method describing buckling of thin-walled structures from global to local loss of stability can be easily adopted in computer-aided systems (CAD/CAM).

The present analysis was completed by including the second approximation in order to investigate post-buckling in the case where the first order interaction is weak.

REFERENCES

Ali, M. A. and Sridharan, S. (1988). A versatile model for interactive buckling of columns and beam-columns. *Int. J. Solids Structures* **24**, 481–486.

Barbré, R. (1936). Beulspannungen in Rechteckplatten mit Langsteifen bei gleichmassiger Druckbeanspruchung. *Der Bauingenieur* **17**, 268.

Benito, R. and Sridharan, S. (1984–85). Mode interaction in thin-walled structural members. *J. Struct. Mech.* **12**, 517–542.

Bernard, E. S., Bridge, R. Q. and Hancock, G. J. (1993). Tests of profiled steel decks with V-stiffeners. *J. Struct. Engng* **119**, 2277–2293.

Biderman, B. L. (1977). *Mechanics of Thin-walled Structures—Statics.* Mashinostroenie, Moscow (in Russian).

Bilstein, W. (1974). Beitrag zur Berechnung vorverformter mit diskreten Längssteifen ausgesteifter, ausschliesslich in Längsrichtung belasteter Rechteckplatten nach der nichtlinearen Beultheorie. *Der Stahlbau* Heft 7 and Heft 9, 193–201, 276–282.

Byskov, E. and Hutchinson, J. W. (1977). Mode interaction in axially stiffened cylindrical shells. *AIAA J.* **15**, 941–948.

Cox, H. L. and Riddell, J. R. (1949). Buckling of a longitudinal stiffened panel. *Aer. Quart.* 1.

Desmond, T. P. (1977). The behaviour and strength of thin-walled compression members with longitudinal stiffeners. Report No. 369, Dept. Struct. Engng, Cornell University, U.S.A.

Hoon, K. H., Rhodes, J. and Seah, L. K. (1993). Tests on intermediately stiffened plate elements and beam compression elements. *Thin-Walled Structures* **16**, 111–143.

Höglund, T. (1978). *Design of Trapezoidal Sheeting Provided with Stiffeners in the Flanges and Webs.* Manus, Stockholm, Sweden.

Klöppel, K. and Bilstein, W. (1971). Ein Verfahren zur Ermittlung der Beullasten beliebiger rechtwinkling abgekanteter offener und geschlossener Profile nach der linearen Beultheorie unter Verwendung eines abgewandelten Reduktionsverfahrens. Veröffentlichungen des Institutes für Statik und Stahlbau der Technischen Hochschule, Darmstadt, Heft 16.

Koiter, W. T. (1963). Elastic stability and post-buckling behaviour. In *Proceedings of the Symposium on Nonlinear Problems*, pp. 257–275. University of Wisconsin Press, Wisconsin.

Koiter, W. T. (1976). General theory of mode interaction in stiffened plate and shell structures. WTHD Report 590, Delft.

Koiter, W. T. and van der Neut, A. (1980). Interaction between local and overall buckling of stiffened compression panels. In *Thin-Walled Structures* (Edited by J. Rhodes and A. G. Walker), part I, pp. 51–56, part II, pp. 66–86. Granada, St Albans.

Kolakowski, Z. (1987a). Mode interaction in thin-walled trapezoidal column under uniform compression. *Thin-Walled Structures* **5**, 329–342.

Kolakowski, Z. (1987b). Mode interaction in wide plate with closed section longitudinal stiffeners under compression. *Engng Trans.* **35**, 591–609.

Kolakowski, Z. (1988). Some aspects of mode interaction in thin-walled stiffened plate under uniform compression. *Engng Trans.* **36**, 167–179.

Kolakowski, Z. (1989a). Interactive buckling of thin-walled beams with open and closed cross-section. *Engng Trans.* **37**, 375–397.

Kolakowski, Z. (1989b). Mode interaction in wide plate with angle section longitudinal stiffeners under compression. *Engng Trans.* **37**, 117–135.

Kolakowski, Z. (1989c). Some thoughts on mode interaction in thin-walled columns under uniform compression. *Thin-Walled Structures* **7**, 23–35.

Kolakowski, Z. (1993a). Influence of modification of boundary conditions on load carrying capacity in thin-walled columns in the second order approximation. *Int. J. Solids Structures* **30**, 2597–2609.

Kolakowski, Z. (1993b). Interactive buckling of thin-walled beams with open and closed cross-sections. *Thin-Walled Structures* **15**, 159–183.

Kolakowski, Z. (1994). On certain aspects of global and local buckling modes in thin-walled columns-beams. *J. Theor. Appl. Mech.* **32**, 409–427.

Konig, L. (1978). Transversely loaded thin-walled C-shaped panels with intermediate stiffeners. Document D7, Swedish Council for Building Research, Sweden.

Krolak, M. (Ed.) (1990). *Post-buckling Behaviour and Load Carrying Capacity of Thin-walled Plate Girders*, p. 553. PWN (Polish Scientific Publishers), Warsaw-Lodz (in Polish).

Manevich, A. I. (1982). Theory of interactive buckling of stiffened thin-walled structures. *Prikl'adnaya Matematika i Mekhanika* T. 46, 2, 337–345 (in Russian).

Manevich, A. I. (1985). Stability of shells and plates with T-section stiffeners. *Stroitel'naya Mekhanika i Raschet Sooruzhenii* No. 2, 34–38 (in Russian).

Manevich, A. I. (1988). Interactive buckling of stiffened plate under compression. *Mekhanika Tverdogo Tela* No. 5, 152–159 (in Russian).

Moellmann, H. and Goltermann, P. (1989). Interactive buckling in thin-walled beams. Part I: theory. Part II: applications. *Int. J. Solids Structures* **25**, 715–728, 729–749.
Pignataro, M. and Luongo, A. (1987a). Asymmetric interactive buckling of thin-walled columns with initial imperfection. *Thin-Walled Structures* **3**, 365–386.
Pignataro, M. and Luongo, A. (1987b). Multiple interactive buckling of thin-walled members in compression. *Proc. Int. Colloq. on Stability of Plate and Shell Structures*, University of Ghent, pp. 235–240.
Roorda, J. (1988). Buckling behaviour of thin-walled columns. *Can. J. Civ. Engng* **15**, 107–116.
Sridharan, S. and Ali, M. A. (1985). Interactive buckling in thin-walled beam-columns. *J. Engng Mech. ASCE* **111**, 1470–1486.
Sridharan, S. and Ali, M. A. (1986). An improved interactive buckling analysis of thin-walled columns having doubly symmetric sections. *Int. J. Solids Structures* **22**, 429–443.
Sridharan, S. and Graves-Smith, T. R. (1981). Postbuckling analyses with finite strips. *J. Engng Mech. Div. ASCE* **107**, 869–888.
Sridharan, S. and Peng, M. H. (1989). Performance of axially compressed stiffened panels. *Int. J. Solids Structures*, **25**, 879–899.
Timoshenko, S. P. (1921). Über die Stabilität versteifter Platten. *Der Eisenbau* **12**, 147–163.
Tvergaard, V. (1973). Imperfections sensitivity of a wide integrally stiffened panel under compression. *Int. J. Solids Structures* **9**, 177–192.
Unger, B. (1969). Elastisches Kippen von beliebig gelagerten und aufgehängten Durchlaufträgern mit einfachsymmetrischen, in Trägerachse veränderlichem Querschnitt und einer Abwandlung des Reduktionsverfahrens als Lösungsmethode. Dissertation D17, Darmstadt.

APPENDIX A

The kinematical and static continuity conditions at the junctions of adjacent plates may be written in the form:

$$
\begin{aligned}
u_{i-1}|^0 &= u_i|^+, \\
w_{i-1}|^0 &= w_i|^- \cos(\varphi) - v_i|^- \sin(\varphi), \\
v_{i+1}|^0 &= w_i|^- \sin(\varphi) + v_i|^+ \cos(\varphi), \\
w_{i+1,y}|^0 &= w_{i,y}|^+, \\
M_{(i-1)y}|^0 - M_{iy}|^+ &= 0, \\
N^*_{(i+1)y}|^0 - N^*_{iy}|^+ \cos(\varphi) - Q^*_{iy}|^+ \sin(\varphi) &= 0, \\
Q^*_{(i+1)y}|^0 + N^*_{iy}|^+ \sin(\varphi) - Q^*_{iy}|^+ \cos(\varphi) &= 0, \\
N^*_{(i+1)xy}|^0 - N^*_{ixy}|^+ &= 0,
\end{aligned}
\tag{A1}
$$

where

$$
\begin{aligned}
M_{iy} &= -D_i(w_{i,yy} + v w_{i,xx}), \\
N^*_{iy} &= N_{iy} + N_{iy} v_{i,y} + N_{ixy} v_{i,x}, \\
Q^*_{iy} &= N_{iy} w_{i,y} + N_{ixy} w_{i,x} - D_i[w_{i,yyy} + (2-v) w_{i,xxy}], \\
N^*_{ixy} &= N_{ixy} + N_{ixy} u_{i,x} + N_{iy} u_{i,y}, \\
\varphi &\equiv \varphi_{i,i+1}.
\end{aligned}
\tag{A2}
$$

The boundary conditions referring to the simply supported beam-columns at both ends are assumed to be:

$$
\begin{aligned}
\sum_i \frac{1}{b_i} \int N_{ix}(x_i = 0, y_i)\,\mathrm{d}y_i = \sum_i \frac{1}{b_i} \int N_{ix}(x_i = l, y_i)\,\mathrm{d}y_i &= \sum_i N^o_{ix}, \\
v_i(x_i = 0, y_i) = v_i(x_i = l, y_i) &= 0, \\
w_i(x_i = 0, y_i) = w_i(x_i = l, y_i) &= 0, \\
M_{iy}(x_i = 0, y_i) = M_{iy}(x_i = l, y_i) &= 0.
\end{aligned}
\tag{A3}
$$

APPENDIX B

The conditions resulting from the variational principle for two longitudinal edges on which a relation between the state vectors is derived using the modified transition matrices method may be written in the form:

$$\int_0^l N_{iy}^* \delta v \, \mathrm{d}x_i = \int_0^l [N_{iy} + N_{iy} v_{i,y} + N_{ixy} v_{i,x}] \delta v \, \mathrm{d}x_i = 0$$

$$\int_0^l N_{ixy}^* \delta u \, \mathrm{d}x_i = \int_0^l [N_{ixy} + N_{ixy} u_{i,x} + N_{i,y} u_{i,y}] \, \delta u \, \mathrm{d}x_i = 0$$

$$\int_0^l M_{iy} \delta w_{i,y} \, \mathrm{d}x_i = -\int_0^l D_i (w_{i,yy} + v w_{i,xx}) \, \delta w_{i,y} \, \mathrm{d}x_i = 0$$

$$\int_0^l Q_{iy}^* \delta w \, \mathrm{d}x_i = \int_0^l \{N_{iy} w_{i,y} + N_{ixy} w_{i,x} - D_i [w_{i,yyy} + (2-v) w_{i,xxy}]\} \, \delta w \mathrm{d}x = 0. \tag{B1}$$

APPENDIX C

The coefficients in the non-linear equilibrium equations (8), a_{ijJ}, are given by the following expression [see Byskov and Hutchinson (1977) for more detailed analysis]:

$$a_{ijJ} = [\sigma^{(J)} \cdot l_{11}(U^{(i)}, U^{(j)}) + 2\sigma^{(i)} \cdot l_{11}(U^{(j)}, U^{(J)})] / (2\sigma^{(J)} \cdot \varepsilon^{(J)}). \tag{C1}$$